Fermi LAT Observations of the Geminga Pulsar

Ozlem Celik*,† **for the *Fermi* LAT Collaboration**

**NASA Goddard Space Flight Center, Greenbelt, MD 20771, USA*
†*Center for Space Science Technology (CRESST), University of Maryland, Baltimore County, Baltimore, MD 21250, USA*

Abstract. **The Geminga pulsar is the second brightest galactic source, and was the first known radio-quiet pulsar. The pulsations from Geminga were first discovered in X-rays by ROSAT, and pulsed gamma-rays were detected by EGRET on CGRO following that. The EGRET measurement of the Geminga emission spectrum was compatible with a power law shape with a fall-off above energies of 2 GeV, although the cutoff energy of the emission could not be determined due to limited statistics at these energies. The Large Area Telescope (LAT) on board the *Fermi Gamma-ray Space Telescope*, launched on 11 June 2008, has unprecedented sensitivity and capabilities in the energy range from 20 MeV up to 300 GeV which allow us to study the Geminga pulsar in greater detail than ever before. We present our preliminary studies on the pulse profile and energy spectrum of the emission from the Geminga pulsar using the *Fermi* LAT data.**

Keywords: **gamma rays, pulsars, Geminga**

I. INTRODUCTION

The Geminga pulsar has a period of 237 ms and a very stable period derivative of 1.1×10^{-14} s s^{-1} as expected for an old pulsar with the characteristic age of 3×10^5 yrs. The spin-down energy loss for the Geminga pulsar is $\dot{E} = 3.26 \times 10^{34}$ ergs s^{-1}, as determined from its period and period derivative. Geminga is the second brightest non-variable galactic source in the γ-ray sky with periodic emission first detected in X-rays [10] by ROSAT, and pulsed γ-rays [3] detected by EGRET. It has pulsed emission also at optical [15] wavelengths but no confirmed radio emission has been detected from this source. Parallax measurements yield a distance of 250^{+120}_{-62} pc [7] with a measurable proper motion [4], [7].

An analysis of the EGRET data showed a two peak light curve above 30 MeV with a peak separation of ∼0.5 in phase [12], [8]. The EGRET measurement of the Geminga emission spectrum between 30 MeV and 2 GeV was compatible with a power law shape; a fall-off was observed above energies of 2 GeV but the cutoff energy of the emission could not be determined due to limited statistics at these energies [8].

With the excellent sensitivity of the Large Area Telescope (LAT), it was possible to obtain a more sensitive light curve and spectrum of this source using data obtained during the first seven months of LAT all-sky survey. This data set contains more than three times the photons collected by EGRET in its nine year lifetime. This paper reports preliminary results of this analysis.

II. OBSERVATIONS

Fermi Gamma-ray Space Telescope was launched on 11 June 2008 and began sky-survey operations in 4 August 2008 after a short checkout and calibration period. The LAT [2] is a pair-production telescope on *Fermi* and is sensitive to γ-rays in the energy range from 20 MeV to more than 300 GeV. It has an ideal design for pulsar studies, with a large effective area (∼8000 cm^2), small dead-time (∼25 μs/event), and improved angular resolution (∼0.8° at 1 GeV). Its a large field of view (∼2.4 sr) combined with its observing mode maps the entire sky every 3hr. These properties enable collection of many photons from a pulsar in a short amount of time with a high signal to noise ratio. The timing chain from the GPS-based satellite clocks through the pulsar analysis software is accurate to < 1 μs [16].

The data set used in the present analysis was collected during the first seven months of LAT nominal science operations, from 3 August 2008 to 3 March 2009. Events classified as diffuse class [2], which have the tightest background rejection, were used in the analysis, excluding events collected when the pulsar was viewed at zenith angle > 105°to the detector axis to remove the excessive background due to the Earth's albedo photons.

III. TIMING ANALYSIS

Since the end of the EGRET mission, the Geminga timing ephemeris has been maintained using occasional observations with XMM-Newton [11], [9]. Once the LAT began taking data, its densely-sampled, high-precision timing observations have become available and we have constructed a timing solution using these data. For this analysis, the photon times were barycentered assuming a constant location for the Geminga pulsar, calculated at the center of the time span of the LAT data set (MJD 54800), using the Geminga position reported by [5] as reference point and accounting for its proper motion described in [7] (after accounting for an error in the definition of μ_α in that paper). Initially, we determined an approximate ephemeris using an epoch-folding search. Then, using that ephemeris we folded ∼ 20 day segments of data and fitted pulse times of arrival (TOAs) using a Fourier-domain cross correlation with a high signal-to-noise template profile. We obtained one TOA from the stare observation during checkout and 12 TOAs
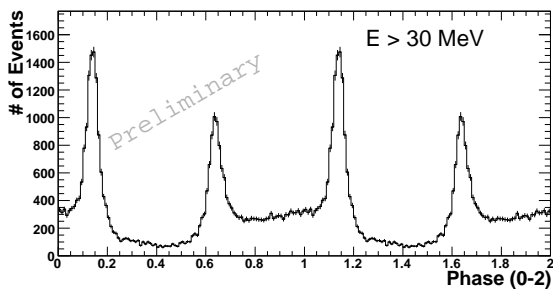
Fig. 1. The pulse profile of the Geminga pulsar for all photons with energies > 30 MeV from a region with radius depending on the angular resolution of the LAT detector, as given in the text. Two pulse periods are shown with a total of 200 constant width phase bins.

from the survey data up to 15 April 2009. We fit these TOAs to a model with only absolute phase, frequency and frequency first derivative as free parameters. The residuals to the model have an RMS of $223\,\mu$s and the model parameters are listed in Table I. Currently, it is not possible to unambiguously align the XMM-Newton X-ray light curve with the *Fermi* LAT profile, but this will become possible once we incorporate the currently proprietary XMM timing observations made contemporaneous with the *Fermi* observation.

TABLE I
THE LAT EPHEMERIS FOR GEMINGA

Parameter	Value
Epoch of position (MJD)	54800
R.A. (J2000)	6:33:54.289
Dec. (J2000)	+17:46:14.38
Epoch of ephemeris T_0 (MJD)	54800
Range of valid dates (MJD)	54662 - 54936
Frequency f (Hz)	4.21756706493(5)
Freq. derivative $\dot{f}$ ($\times 10^{-13}$ Hz s^{-1})	-1.9527(2)
Freq. 2nd derivative $\ddot{f}$ (Hz s^{-2})	0

IV. RESULTS

A. Pulse Profile

The angular resolution of the LAT depends on the reconstructed energy, and accordingly an energy dependent radius of $\theta_{68} \approx 0.8° E_{GeV}^{-0.75}$ is estimated to contain 68% of events. The pulse profile of the Geminga pulsar was reconstructed with photons selected from a region around the Geminga pulsar with radius depending on the LAT angular resolution as $\theta < Max(\theta_{68}, 0.35°)$ in order to include only the photons that can be strongly associated with the source.

In this energy dependent aperture we have 33,363 photons with energies > 30 MeV. Figure 1 shows the pulse profile for two complete pulsar rotation phases with a total of 200 bins. Statistical errors on each bin are also shown, barely larger than the line thickness. The pulse profile shows two strong, sharp peaks separated by 0.502 ± 0.001 in phase. As mentioned in the previous section the location of the phase 0 is not aligned to any
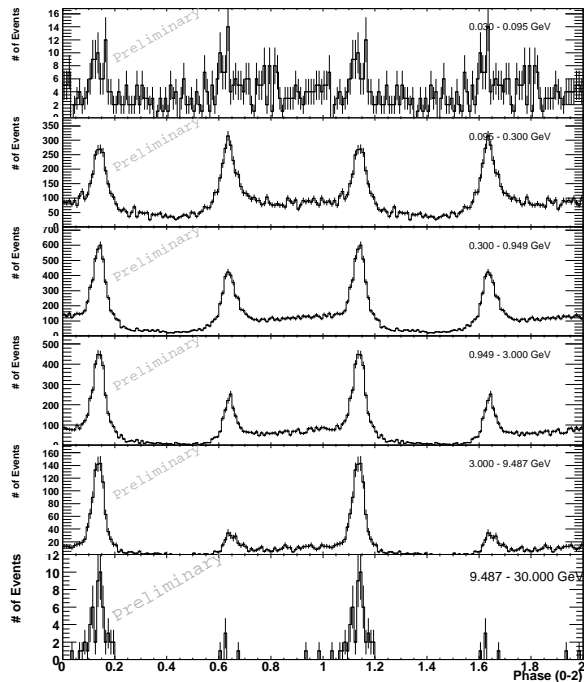

Fig. 2. The energy dependence of the Geminga pulse profile for the same photons in Figure 1 is shown with 2 energy bands per decade.

pulse profiles obtained with other instruments. The peaks were fitted with Lorentzian functions over the phase intervals $0.6 - 0.68$ (P1) and $0.10 - 0.18$ (P2) avoiding the bridge and off-pulse regions. The peaks are fairly narrow, with Lorentzian FWHM for P1 of 0.070 ± 0.003 and for P2 of 0.063 ± 0.002. The first peak has an indication of a slight asymmetry with a steeper outer edge while the second peak has a relatively symmetric shape, but both peaks have long tails into the "off-pulse" region.

Figure 2 shows the energy evolution of the same pulse profile in 2 logarithmically separated energy bands per decade between 30 MeV and 30 GeV. The highest energy photon from the selected region has an energy of 25.6 GeV at the phase of 0.15. All photons > 10 GeV are detected at the phase ranges of the pulsed emission peaks with no detected photons between the peaks. Although the lowest energy band suffers from a high contamination of photons from the diffuse background due to the large selection region, the peaks are still visible. The most prominent feature in the energy evolution is a decrease of P1 relative to P2 with increasing energy as shown in Figure 3 for the energy bands between 0.1 and 10 GeV. Current statistics limit a good fit to the peaks in the lowest and highest energy bands shown; thus they are not included on this plot.

B. Spectrum

Phase-averaged spectral analysis of the Geminga pulsar was performed using the *gtlike* tool, which is a part of the *Fermi* ScienceTools package and employs standard maximum-likelihood methods for spectral es-
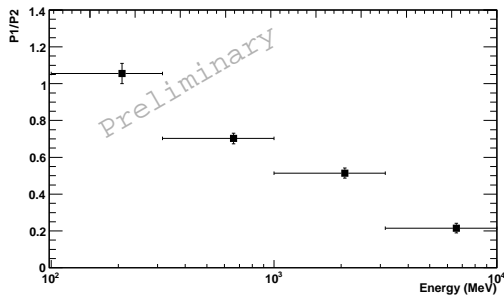
Fig. 3. The energy evolution of the peak ratio P1/P2 is shown for energy bands between 100 MeV and 10 GeV from Figure 2.
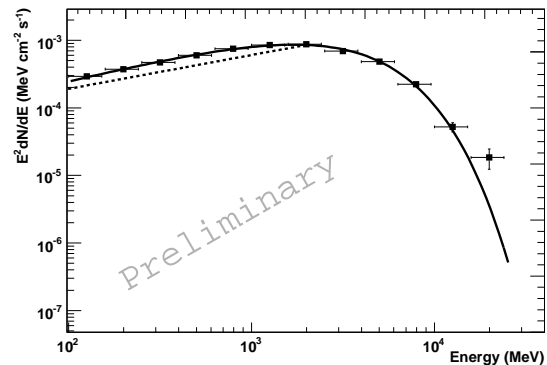

Fig. 4. The phase-averaged spectral energy distribution of the Geminga Pulsar is shown. The solid curve is the best fit spectral form of a power law with a simple exponential cut-off to the LAT data. The dashed line is the spectrum fit by EGRET up to 2 GeV [12]. The square points are obtained by independent fits at each energy bin to the LAT data as described in the text. Only the statistical errors are shown.

timation. This tool fits a model describing the point sources and diffuse emission components present in the region of interest to the data. For this spectral analysis, we selected a data set that includes all photons with energies above 100 MeV in the 20° region around the position of the Geminga pulsar. We modeled the galactic diffuse background using the maps based on GALPROP model [17], [18], and modeled the instrumental and extragalactic diffuse background as isotropically distributed with a power law spectral component. Furthermore, 17 nearby sources in the 20° region that are present in the bright source list [1] are also modeled as point sources with a power law spectrum. Finally, we modeled the Geminga pulsar as a point source with a spectral form of a power law with an exponential cutoff, $dN/dE = N_0(E/1\,GeV)^{-\Gamma}e^{-(E/E_c)}$, where N_0 is the normalization, Γ is the photon index and E_c is the cut-off energy. The fit of this model to the data, allowing all spectral parameters in the model to be free, gives a photon index of 1.337 ± 0.008 and a cut-off energy of $2.563 \pm 0.035\,GeV$ for the Geminga pulsar. An integral photon flux of $(4.28 \pm 0.03) \times 10^{-6}\,cm^{-2}s^{-1}$ and an integral energy flux of $(4.18 \pm 0.03) \times 10^{-9}\,ergs\,cm^{-2}s^{-1}$ are obtained for the energy range of $0.1 - 300\,GeV$. All the errors are statistical. The systematic errors are due to the uncertainties in the energy dependent effective area and they are currently under investigation. In order to check the assumption of a cut-off energy in the spectrum, we have also fit the same data set modeling the spectral component of the Geminga pulsar with a simple power law. From the comparison of the log likelihood values of both fits, the power law hypothesis for the Geminga spectrum was rejected by $>70\sigma$ in favor of an exponential cutoff using the likelihood ratio test. Similarly, a power law with a super-exponential cutoff form, $dN/dE = N_0(E/1\,GeV)^{-\gamma}exp(-(E/E_c)^b)$, was tested for $b > 1$ and it was rejected at $\sim 20\sigma$ level for b=2 in favor of a power law with a simple exponential cut-off form.

Figure 4 plots the differential energy flux spectrum, E^2dN/dE, of the Geminga pulsar obtained from the best fit model for energies above 100 MeV. The spectrum fit to the EGRET data in the energy range up to 2 GeV [12]

is also shown as a dashed line. In order to obtain the points on the LAT spectrum, a similar fitting method was applied independently in each energy bin defined by the horizontal error bars. Assuming in a sufficiently small energy bin a spectrum of any form can be approximated by a simple power law with a photon index of 2, the data were divided into 5 energy bins per decade in log(Energy) and the fit was performed by modeling all the point sources with this spectral form allowing only the normalization parameters as free. When a nearby source was not detected above 5σ in an energy bin, its normalization was fixed at the level expected in that energy bin from the fit over the full energy range and the fit was repeated. The spectrum points obtained with this method for Geminga agree well with the overall fit up to 16 GeV. We are investigating the reasons for the discrepancy between the spectral point and the overall curve on the last energy bin to determine whether it is an effect of low statistics, our fitting method, or an indication of a separate component in the light curve with a harder spectrum compared to the phase-averaged spectrum which is a superposition of the distinct components. Further analysis to produce a phase-resolved spectrum of the source to study physically distinct emission regions with different spectral properties is ongoing. In the energy bins above 25 GeV, Geminga was not detected above the 5σ level with the current statistics.

C. Search for a Nebular Component

It is seen from the total and energy dependent light curve that the pulsed emission extends over a wide phase range with long tails into the phase range between 0.25 and 0.55. Moreover, there are no photons above 3 GeV inside the 68% containment radius around the source between phases 0.4 and 0.5. This phase region was designated as the most stringent off-pulse region for the pulsar and energy dependent photon count maps were

generated for this range around the Geminga position to check if any localized excess emission is present over the diffuse background. A point source excess was significantly detected at the location of the Geminga pulsar in this off-pulse phase range above $> 100\,\mathrm{MeV}$ up to 1 GeV, but there is no indication of an excess emission above 1 GeV. The spectrum of the emission over this off-pulse region was measured and it was found that a power law emission with an exponential cut-off consistent with the pulsed emission is favored (with the current statistics) over a simple power law spectrum expected from a possible nebular emission. This result suggests that all the emission detected from the Geminga pulsar is completely pulsed and covers the whole phase range. Further analysis is ongoing with increased statistics to infer whether any nebular component is present around the Geminga pulsar or to put upper limits on its existence if no detection is possible.

V. DISCUSSION

The high statistics obtained from the LAT data has significantly improved the precision in the pulse profiles of Geminga and has increased the high energy sensitivity significantly for determination of the overall spectral shape of the high energy pulsed emission. The combination of these factors contributes greatly in distinguishing between the high energy pulsed emission models.

The maximum energy of the pulsed photons from Geminga, 25 GeV, defines the lower threshold of the magnetic pair production in the pulsar environment, and in turn predicts the lower bound for the emission altitude. The maximum observed energy of pulsed photons combined with the magnetic field strength and $\dot{P}$ of Geminga favors a high altitude of the emission. The statistical preference for a simple exponential cut-off form on the spectrum as opposed to a super-exponential cut-off form also supports the high altitude models like outer gap (OG) [6], [14] or slot gap (SG) [13] and precludes emission very near the stellar surface.

Furthermore, the number of main peaks and the peak separation can be used to constrain the geometry of the emission, i.e. the magnetic inclination and viewing angles α and ζ and the flux correction factor f, which in turn give hints on the underlying emission model. According to the "Atlas" of light curves in [19], one can use the pulsar spin-down power to estimate the width of the emission gap w and the γ-ray efficiency $w \equiv \eta \simeq (10^{33}\mathrm{ergs\,s^{-1}}/\dot{\mathrm{E}}_{\mathrm{SD}})^{1/2}$. With this assumption w can be estimated as 0.175 for the Geminga pulsar. Using the "Atlas" [19] for this gap width, a peak separation of 0.5 in phase and the absence of a radio emission from Geminga, OG models are allowed by a very constrained phase space of $\alpha \sim 10° - 25°$ and $\zeta \sim 85°$ predicting f$\sim 0.1 - 0.15$. The SG models on the other hand are allowed by a relatively relaxed geometry of $\alpha \sim 30° - 80°$, $\zeta > 80°$ and $\alpha > 80°$, $\zeta \sim 55°75°$ predicting f as > 0.5.

The γ-ray efficiency of a pulsar can also be estimated from the total γ-ray luminosity, $\mathrm{L}_\gamma = 4\pi\mathrm{f}(\alpha,\zeta)\Phi_{\mathrm{obs}}\mathrm{d}^2$, where f is the flux correction factor depending on the geometry, Φ_{obs} is the observed phase-averaged energy flux, and d is the distance to the source. Using the Geminga parallax distance of 250 pc and the measured energy flux, we obtain a total luminosity of $\mathrm{L}_\gamma = 3.16 \times 10^{34}\mathrm{f}$ ergs s^{-1} for Geminga. The γ-ray efficiency $\eta = \mathrm{L}_\gamma/\dot{\mathrm{E}}_{\mathrm{sd}}$ is thus obtained as $0.88\,\mathrm{f}$. Combining with the former assumption of the γ-ray efficiency relation by [19], one obtains a value of ~ 0.2 for the flux correction factor with an uncertainty of about a factor of 2 due to the large error on the distance measurement. The predictions of OG and SG models are consistent with this value of f within the uncertainty in the distance.

Additionally, the Geminga pulsar is not detected in radio energy range, but the γ-ray pulsed emission is seen over a wide phase range, with almost no off-pulse region in the light curve. This suggests that the radio pulse, if exists, beams in a very narrow angle away from our line of sight while the γ-ray beam covers a large fraction of solid angle of the sky. The presence of pulsed emission over the entire phase range requires that the emission exists below the null-charge surface in outer magnetosphere models, constraining the geometry of the OG models severely.

VI. ACKNOWLEDGMENT

REFERENCES

[1] Abdo, A. A. *et al.* 2009, submitted to ApJS, arXiv:0902.1340
[2] Atwood, W.B. *et al.* 2009, accepted by ApJS, arXiv:0902.1089
[3] Bertsch, D. L. *et al.* 1992, Nature, 357, 306
[4] Bignami, G. F. *et al.* 1993, Nature, 361, 704
[5] Caraveo, P. A. *et al.* 1998, A&A, 329, 1
[6] Cheng, K. S. *et al.* 1986, ApJ, 300, 500
[7] Faherty, J. *et al.* 2007, Ap&SS, 308, 225
[8] Fierro, J. M. *et al.* 1998, ApJ, 494, 734
[9] Halpern, J. P., private communication
[10] Halpern, J. P. & Holt, S. S. 1992, Nature, 357, 222
[11] Jackson, M. S. & Halpern, J. P. 2005, ApJ, 633, 1114
[12] Mayer-Hasselwander, H. A. *et al.* 1994, ApJ, 421, 276
[13] Muslimov, A. G. & Harding, A. K. 2004, ApJ, 606, 1143
[14] Romani, R. W. & Yadigaroglu, I. A. 1995, ApJ, 438, 314
[15] Shearer, A. *et al.* 1998, A&A, 335, L21
[16] Smith, D. A. *et al.* 2008, A&A, 492, 923
[17] Strong, A. W. *et al.* 2004, ApJ, 613, 962
[18] Strong, A. W. *et al.* 2004, A&A, 422, L47
[19] Watters, K. P. *et al.* 2009, ApJ, 695, 1289